Materials Horizons

ROYAL SOCIETY OF CHEMISTRY

COMMUNICATION

View Article Online
View Journal | View Issue

Cite this: *Mater. Horiz.*, 2021, 8, 1454

Received 4th October 2020,
Accepted 15th December 2020

DOI: 10.1039/d0mh01582b

rsc.li/materials-horizons

Metabolically engineered bacteria as light-controlled living therapeutics for anti-angiogenesis tumor therapy†

Xingang Liu,‡[a] Min Wu,‡[a] Meng Wang,[b] Yukun Duan,[a] ChiUyen Phan,[c] Guobin Qi,[a] Guping Tang *[c] and Bin Liu *[ad]

A living therapeutic system based on attenuated *Salmonella* was developed *via* metabolic engineering using an aggregation-induced emission (AIE) photosensitizer MA. The engineered bacteria could localize in the tumor tissues and continue to colonize and express exogenous genes. Under light irradiation, the encoded VEGFR2 gene was released and expressed in tumor tissues, which can suppress angiogenesis induced by a T cell-mediated autoimmune response and inhibit tumor growth.

New concepts

Living bacteria therapeutic systems are living factories that autonomously self-replicate, generate and pump out therapeutics inside the body. The main limitation of living bacteria therapy is the inefficient release of therapeutics from bacteria, especially for bactofection delivery of therapeutic genes, which mostly depends on spontaneous lysis or exogenous molecules, making it difficult to realize on-demand control of the process. Herein, a living therapeutic system was developed based on attenuated *Salmonella via* metabolic engineering using an aggregation-induced emission (AIE) photosensitizer **MA** to realize light-controlled gene release for breast cancer therapy. The labeling of **MA** does not inhibit *Salmonella* reproduction so that the administered **MA**-engineered *Salmonella* carrying vascular endothelial growth factor receptor 2 (VEGFR2) plasmids can be localized in the tumor tissues and continue to colonize and express exogenous genes. Following an appropriate treatment schedule, the constructed plasmid could undergo controlled-release into the cytoplasm of the host cells under light irradiation. The designed expression of VEGFR2 proteins could then block the immunological tolerance to VEGFR2 and induce a T cell-mediated autoimmune antiangiogenic response. Through a series of *in vitro* and *in vivo* experiments, prominent tumor suppression performance was validated with the engineered living therapeutic system, demonstrating its great potential in precise tumor treatment.

Introduction

Engineered living therapeutic systems are renowned as the next generation of therapeutics for a broad range of indications from treating and preventing infections to suppressing tumors and curing metabolic disorders.[1] Compared with traditional systemic treatment such as gene delivery systems mediated by viral and non-viral vectors, living therapeutics serve as factories that autonomously self-replicate, generate and pump out therapeutics inside the body.[2] The use of live bacteria as living therapeutics for cancer regression has been recognized and practiced, in which programmable attenuated bacterial strains express extraneous genes or generate products *in vitro* and *in vivo* like enzymes, proteins, and immunotoxins.[3,4] Although bacteria have been used as therapeutic agents for many years, pathogenic effects and ineffective therapeutic drug release from intracellular bacteria are issues that remain to be addressed.

Taking an intracellular live bacterium, attenuated *Salmonella*, as an example, it has many desirable properties, such as specific tumor targeting, and being able to proliferate inside tumor tissues and induce tumor regression.[5–8] Genetically engineered *Salmonella* is able to deliver therapeutic proteins or produce therapeutic cytokines, tumor-specific antigens, and antibodies or transfer genes in eukaryotic vectors for bactofection.[9] The main shortcoming of the *Salmonella* strategy is the ineffective therapeutic drug release from the intracellular bacteria, especially for bactofection delivery of therapeutics genes. Bactofection is a method of using bacteria as a vector to deliver genes directly into the target cells *in vivo*.[10–12] After the bacteria enter the target cells, the plasmid encoding the therapeutic gene is released and finally

[a] *Department of Chemical and Biomolecular Engineering, National University of Singapore, Engineering Drive 4, 117585, Singapore. E-mail: cheliub@nus.edu.sg*
[b] *Department of Hepatobiliary and Pancreatic Surgery, First Affiliated Hospital, Zhejiang University, School of Medicine, Hangzhou 310003, China*
[c] *Department of Chemistry, Zhejiang University, Hangzhou 310028, China. E-mail: tangguping@zju.edu.cn*
[d] *Joint School of National University of Singapore and Tianjin University, International Campus of Tianjin University, Binhai New City, Fuzhou 350207, China*

† Electronic supplementary information (ESI) available. See DOI: 10.1039/d0mh01582b

‡ These authors contributed equally to this work.

transferred into the cell nucleus, where the therapeutic gene is expressed by the host cell's expression system. Currently, gene release from intracellular bacteria is mostly dependent on spontaneous bacterial lysis or exogenous molecules to trigger drug release by membrane degradation, which may cause undesirable side effects on the body and cannot be controlled on demand.[13,14] Programed lysis of bacteria based on lysis genes is a promising solution, but it requires more complex genetic engineering of *Salmonella*, which adds time and cost for the process.[1] Therefore, a simple and biocompatible system with controlled gene release is vital for living bactofection therapeutics.

Vascular endothelial growth factor receptor 2 (VEGFR2) is overexpressed in activated endothelial cells during angiogenesis in the tumor vasculature, which plays an important role in tumor growth, invasion and metastasis.[15] Therefore, it can be applied as a potential therapeutic target for anti-angiogenesis and tumor growth suppression.[16–19] In the present study, we construct a living therapeutic system based on attenuated *Salmonella* (strain VNP20009) with light controlled VEGFR2 gene release ability, which can suppress angiogenesis induced by a T cell-mediated autoimmune response against self-antigens expressed by proliferating endothelial cells. As shown in Scheme 1, VEGFR2 plasmid transduced live *Salmonella* can be engineered by a metabolic labeling strategy with MeTTPy-D-Ala (**MA**). **MA** exhibits low emission in aqueous media due to the hydrophilicity of pyridinium and D-Ala. The far-red/near-infrared (FR/NIR) fluorescence would turn on once the MA molecules were attached to bacterial peptidoglycan through metabolic labeling.[20,21] The metabolically incorporated MA can also serve as a photosensitizer to generate ROS under light irradiation. VNP20009 is a bacterial strain genetically modified by depleting the purI genes, creating an auxotrophic mutant for adenine that bacteria can obtain from necrotic areas inside tumors, making bacteria replication more tumor-specific.[22,23] As tumor-targeting bacteria, the intravenously administered MA-engineered *Salmonella* carrying VEGFR2 therapeutic plasmids can be localized in the tumor tissues and continue to colonize and express exogenous genes. Applying light irradiation would destruct the bacteria cell membrane by generating singlet oxygen ($^1O_2$) from MA to facilitate on-demand plasmid release into the host cell cytoplasm. The released plasmid could express the VEGFR2 protein inside the host cells, which is considered as a foreign antigen to break immunological tolerance to VEGFR2 and induce a T cell-mediated autoimmune antiangiogenic response leading to the suppression of tumor growth.[24–26]

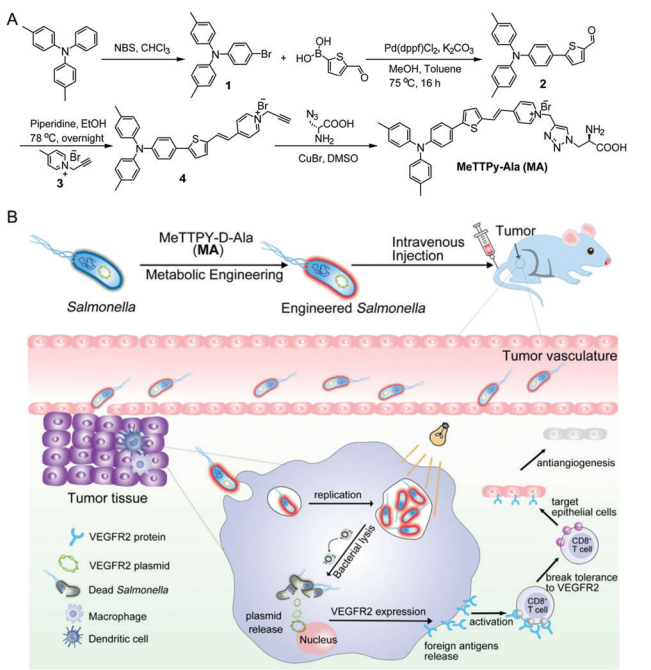

Scheme 1 Schematic illustration of (A) the synthetic route to target compound **MA** and (B) *Salmonella* encoding the VEGFR2 plasmid engineered with **MA** and its anti-angiogenesis therapy of breast cancer *in vivo*.

Results and discussion

The synthetic route to **MA** is shown in Scheme 1A. Briefly, 4,4′-dimethyltriphenylamine was brominated with *N*-bromosuccinimide (NBS) and further reacted with 5-formyl-2-thienylboronic acid *via* a Suzuki reaction to give compound **2** in 71% yield. A Knoevenagel condensation reaction between compounds **2** and **3** yielded the intermediate compound **4**, which was further reacted with D-Ala *via* a copper(I)-catalyzed azide–alkyne cycloaddition reaction to give **MA** in 32% yield. The chemical structures of **MA** and the intermediates were well characterized by NMR and mass spectroscopy (Fig. S1–S6, ESI†) and the purity was verified by reverse-phase HPLC (Fig. S7, ESI†).

MA has a donor–π–acceptor (D–π–A) structure comprised of methyl substituted triphenylamine (as the D), thiophene (as the D and π bridge), a carbon–carbon double bond (as the π bridge) and pyridinium (as the A), which shows an absorption peak at 480 nm and maximum emission located at 710 nm in DMSO/water (v/v = 1/99) solution (Fig. 1A). As shown in Fig. 1B, **MA** has low fluorescence when the fraction of poor solvent toluene is between 0 and 70% but becomes highly emissive when 90% (v/v) of toluene is added, which displays a typical AIE property. **MA** also shows photosensitizing capability to generate singlet oxygen ($^1O_2$).[27] The ROS generation capacity of **MA** was evaluated using 9,10-anthracenediyl-bis(methylene)dimalonic acid (ABDA) as the indicator, which was further compared with commercial photosensitizer Rose Bengal. As shown in Fig. 1C and Fig. S8 (ESI†), the degradation rate of ABDA was about 15 nmol min^{-1} by **MA** and 10 nmol min^{-1} by Rose Bengal under the same light illumination (30 mW cm^{-2}), revealing highly effective $^1O_2$ production capability of **MA**.

We next investigated whether **MA** could be used to label bacteria through a metabolic pathway. After incubating *Salmonella* cells with **MA** (20 μM) for 30 min, almost all the bacteria were effectively labeled by **MA** without any washing procedure needed (Fig. 1D). The covalent ligation of **MA** in peptidoglycan was further validated by MALDI-TOF mass analysis of **MA**-treated *Salmonella* cell lysate (Fig. S9, ESI†). **MA** was anticipated to be included in the peptidoglycan

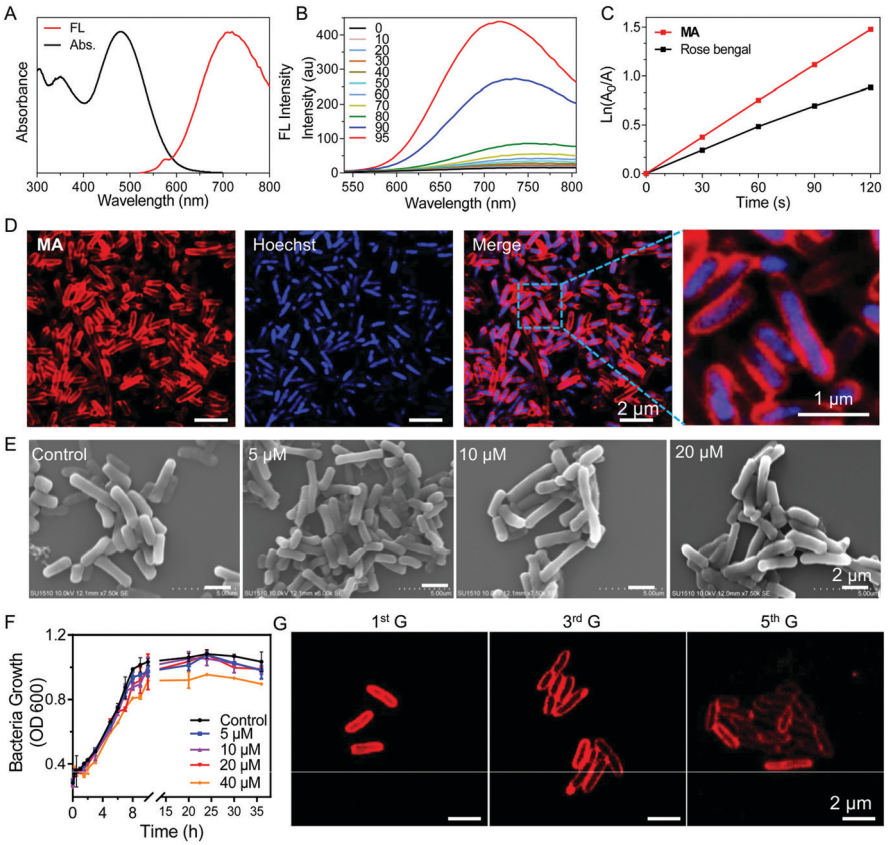

Fig. 1 (A) Normalized absorption and fluorescence (FL) spectra of **MA** in DMSO and water (v/v = 1/99) solution. (B) FL spectra of **MA** (10 μM) in DMSO/toluene mixtures with different toluene fractions (v:v); λ_{ex}: 488 nm. (C) Decomposition rates of ABDA induced by ROS generated from **MA** (10 μM) under white light irradiation (30 mW cm^{-2}) in DMSO/water (v/v = 1/99) solution. [ABDA] = 5 × 10^{-5} M, time interval for recording the UV-vis spectra: 30 s. (D) Confocal microscopy images of metabolically labelled *Salmonella* (20 μM **MA** for 30 min). (E) Field emission scanning electron microscopy images of *Salmonella* labelled with various concentrations of **MA**. The control group is the untreated *Salmonella*. (F) The bacterial growth of **MA** labelled *Salmonella* in fresh LB solution. (G) Confocal microscopy images of **MA** labelled *Salmonella* at different cell generation cycles in fresh LB solution.

biosynthesis process, during which **MA** would be inserted into bacterial peptidoglycan to emit strong fluorescence as a result of the restricted intramolecular motions.[15] Interestingly, when compound **4** without the D-Ala segment was used as a control to label *Salmonella*, no light-up fluorescence was observed (Fig. S10, ESI†). **MA** release assay from **MA**@SV conducted in PBS at 37 °C also showed the excellent stability of **MA**@SV (Fig. S11, ESI†). These indicated that the red signal was produced from metabolically labeled bacteria but not by nonspecific interactions. When *Salmonella* was incubated with various concentrations of **MA** for 30 minutes, the confocal images (Fig. S12, ESI†) and flow cytometric analysis (Fig. S13, ESI†) results were observed to be dose dependent. As the *Salmonella* upon incubation with 20 μM of **MA** showed the highest brightness, 20 μM was selected as the optimal concentration to label *Salmonella* in the following experiments. Meanwhile, **MA** labeling of *Salmonella* was noticed to be time-dependent and most bacteria were stained effectively in 30 min (Fig. S14, ESI†).

To evaluate whether the metabolic labeling method would affect the functions of *Salmonella*, scanning electron microscopy (SEM) was used to observe the bacteria morphology after **MA** labeling. *Salmonella* displayed a typical rod form with a smooth membrane exterior when labeled with 5–20 μM **MA**, and no significant morphological changes were found in the SEM images compared with the control *Salmonella* (Fig. 1E). No nanoaggregates were found to adhere on the surface of **MA**-labeled *Salmonella* (*Salmonella* VEGFR2@**MA**, or, for short, SV@**MA**), indicating that **MA** dissolved well and existed as a monodisperse molecule at 5–20 μM in aqueous media.

As a living therapeutic system, the ability of the engineered *Salmonella* to autonomously self-replicate and produce the therapeutic inside the body is critical for disease treatment. Therefore, the effect of the **MA** labeling method on bacterial growth was studied with various concentrations of **MA**. As shown in Fig. 1F, the growth curve of *Salmonella* clearly described the lag, log and stationary phase at a concentration of 20 μM, demonstrating that **MA** exerted no significant inhibitory effects on the growth of *Salmonella*. After SV@**MA** growing in fresh LB solution for 5 generations, bright red fluorescence could still be observed on the cell membrane of each bacterium (Fig. 1G), indicating that **MA** metabolic labeling is a biocompatible and lasting engineering method for construction of a living therapeutic system.

The inefficient release of therapeutic genes from bacteria into the host cells is an obstacle faced in bactofection due to the weak membrane crossing of genes in the majority of cases.

Recent papers revealed that the bacterial membrane can be damaged by ROS generated from membrane-bound photosensitizers.[28–30] We next studied whether the **MA** engineering method could facilitate therapeutic gene release. Firstly, live/dead co-staining assays were performed. When labeled with 5–20 μM **MA**, most *Salmonella* remained alive in the dark (Fig. 2A), indicating good biocompatibility of the staining method. Under light irradiation (30 mW cm^{-2}) for 10 min, substantial cell death was caused by the generated ROS from **MA** (Fig. 2A), which resulted in a high level of bacterial membrane weakening with 20 μM SV@**MA** (Fig. 2B). The live and dead assay results demonstrated that the ROS generation of intracellular SV@**MA** would not contribute to cytotoxic effects on the host cells (Fig. S15, ESI†). Since extensive bacterial membrane damage was verified, the supernatant absorbance at 260 nm was detected to allow quantification of the released DNA.[31] Concentration-dependent release profiles were observed in DNA release (Fig. 2C), where the amount of DNA released in 20 μM labeled SV@**MA** was 1.5-fold higher than that of 5 μM labeled SV@**MA** and 9-fold higher than that of the control *Salmonella*, showing an effective light-controlled gene release capability. The cellular uptake of SV@**MA** by 4T1 cells (murine breast cancer cell line) was analyzed with fluorescence microscopy. Red signals were observed in the cytoplasm of 4T1 cells in the confocal images (Fig. 2D) and the transmission electron microscope (TEM) images of ultrathin cell slices showed that SV@**MA** was able to invade eukaryotic cells (Fig. 2E). Next, protein expression of VEGFR2 was confirmed by western blotting of transfected 4T1 cells (Fig. 2F). The SV@**MA** treated cells with light irradiation showed 4-fold higher VEGFR2 expression compared with the other groups (Fig. 2G). These results collectively demonstrate that SV@**MA** is able to enter the target cells and realize light-controlled plasmid DNA release and protein expression inside the target cells.

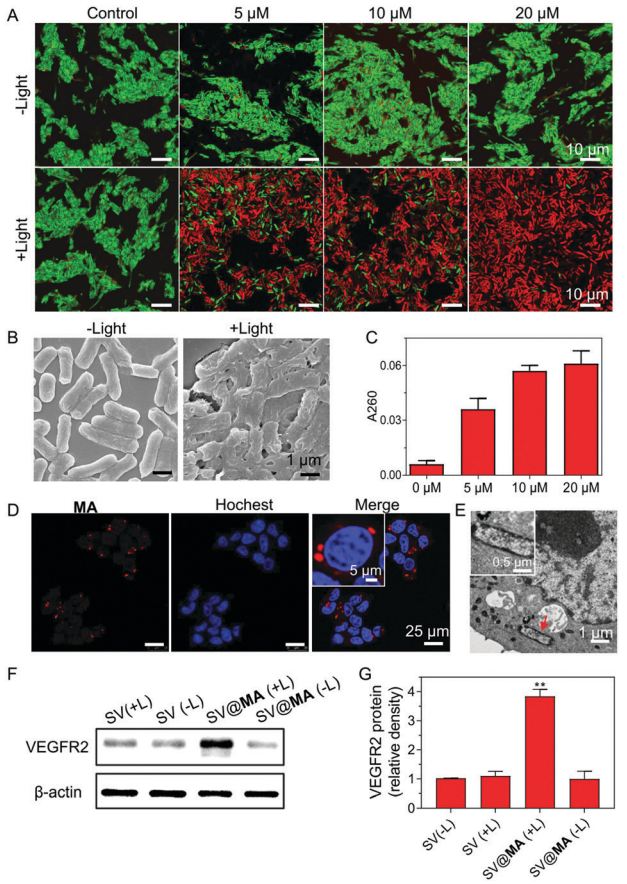

Fig. 2 (A) Live and dead assays of *Salmonella* stained with different concentrations of **MA** with or without white light irradiation (30 mW cm^{-2}, 10 min). (B) Field emission scanning electron microscopy images of SV@**MA** (20 μM) with or without light irradiation (30 mW cm^{-2}, 10 min). (C) DNA release studies of *Salmonella* stained with different concentrations of **MA** with light irradiation (30 mW cm^{-2}, 10 min). (D) Confocal fluorescence images of 4T1 cells incubated with SV@**MA** for 4 h. (E) TEM images showing the intracellular position of SV@**MA** in the ultrathin cell slices of 4T1 cells. (F) Western blot analysis of VEGFR2 expression in 4T1 cells after different transfection treatment. Light irradiation: 30 mW cm^{-2}, 10 min. (G) Quantitative analysis of VEGFR2 protein expression in 4T1 cells after different treatment.

Encouraged by the effective proliferation and light-controlled gene release capability of the living SV@**MA** therapeutic system *in vitro*, we then investigated whether the labeled *Salmonella* could be used as a bactofection vehicle *in vivo*. BALB/c mice were subcutaneously inoculated with 4T1 cells at the right abdomen, where tumors were allowed to grow to a volume of approximately 100 mm^3. Fig. 3A shows the detailed treatment schedule. The tumor targeting efficacy of SV@**MA** was evaluated by monitoring the fluorescence signal of **MA** using an IVIS spectrum imaging system. As shown in Fig. 3B, **MA** showed unsatisfactory tumor targeting capacity, and was mainly distributed in the liver and kidneys. A notable fluorescence signal was observed in the tumor area 4 h post-injection of SV@**MA** (Fig. 3C and Fig. S16, ESI†), demonstrating the intrinsic tumor-targeting capability of **MA**-labeled *Salmonella*. Next, the amount of *Salmonella* in tumors was respectively counted at days 1, 3, 7 and 22 after intravenous injection of SV@**MA**. At day 3 before the 1st light irradiation, the bacterial concentration in tumor tissue was increased 2.6-fold compared to that on day 1 (Fig. 3D),[32,33] indicating that the bacteria retain their proliferation characteristics in the target tissue. After the 2nd light irradiation treatment, the bacterial concentration in tumors at day 7 was reduced dramatically as compared with that of day 3 and subsequently became undetectable at day 22 (Fig. 3E). This was due to the bacterial death caused by the light-generated ROS followed by body clearance. However, the bacteria in tumors of the SV@**MA**(−L) and SV(+L) treated mice multiplied to significantly higher bacterial contents at day 7 (Fig. S17, ESI†). The above results indicate that SV@**MA** could preferentially accumulate and proliferate to a high level in tumor tissues, and the bacterial growth could be inhibited in a light-controlled manner.

Under light irradiation, the ROS generated from SV@**MA** was expected to destroy the bacterial membrane, and cause the release of therapeutic plasmids into the host cells.[34] Western blotting was used to analyse the protein expression of the released plasmid inside the host cells (Fig. 3F). There was an increase in VEGFR2 expression in SV@**MA**(+L) treated tumors, which was 5.0-fold and 1.6-fold higher than the PBS and

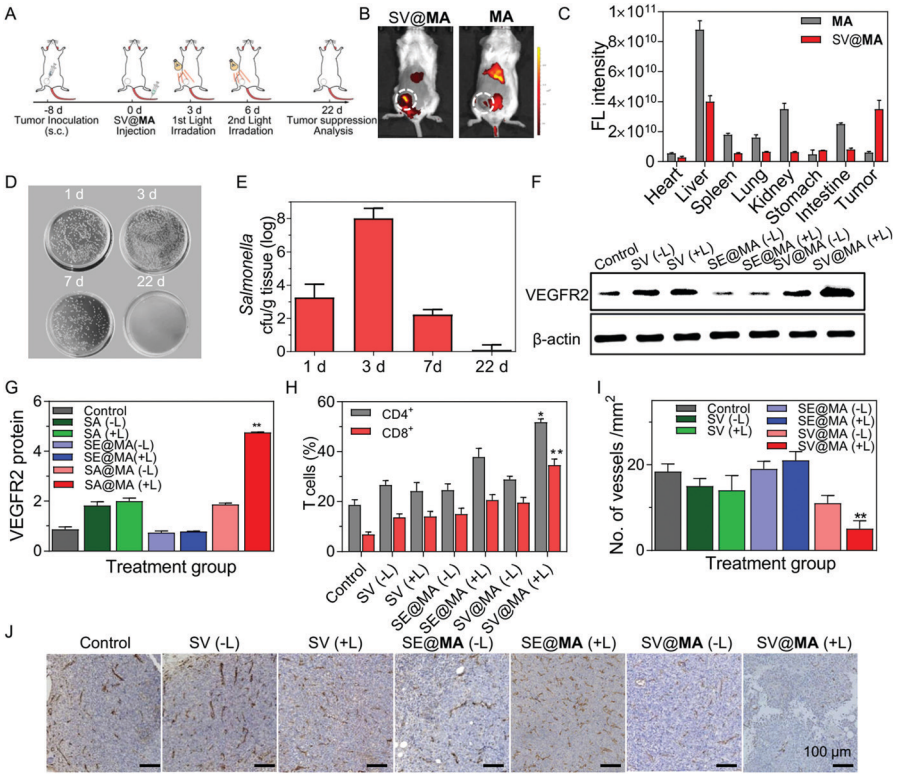

Fig. 3 (A) Schematic illustration of the treatment schedule for anti-angiogenesis tumor therapy mediated by SV@**MA** in a 4T1 tumor model. (B) Fluorescence imaging of the SV@**MA** and **MA** distributions in 4T1 tumor-bearing BALB/c mice *in vivo*. Fluorescence images were taken 4 h after the mice were injected with SV@**MA** or **MA**. (C) Average fluorescence intensities in main organs and tumor tissues 4 h after intravenous injection of SV@**MA** or **MA** (n = 3). (D) Selective *Salmonella* growth and (E) *Salmonella* counts in tumor tissues. Tumor tissue homogenates of SV@**MA**(+L) at different days were cultured on solid LB agar at 37 °C for 24 h. 1 d and 3 d represent the 1st and 3rd day after injecting SV@**MA**. 7 d and 22 d represent the 1st and 14th day after the second light irradiation. (F) Western blot analysis and (G) quantification of VEGFR2 protein expression in tumor tissue after treatment with different formulations (n = 5). (H) Quantitative flow cytometry analysis of $CD4^+$ and $CD8^+$ T cells in 4T1 tumor model BALB/c mice immunized with different formulations. The cells were isolated from the blood and stained with FITC-CD4 and PE-CD8 antibodies. (I) Quantification and (J) immunohistochemical analysis of CD31 in the tumor slices of the 4T1 tumor model at day 22 after treating with different formulations.

SV@**MA**(−L) treated group (Fig. 3G), respectively, indicating the high-efficiency of controlled gene release and expression under light irradiation.

Normally, the tumor vascular epithelial cells are immune tolerant to T cell killing due to the down-regulation of major histocompatibility (MHC) antigens required for T cell-mediated antitumor responses in tumors.[35,36] Several preclinical studies have shown that xenogenic VEGFR2 as a foreign antigen can break the immunological tolerance against VEGFR2 and evoke an antiangiogenic response by inducing a T cell-mediated immune response against VEGFR2 overexpressed endothelial cells in the tumor vasculature.[24–26,37] Here, we explored the potential of expressed VEGFR2 proteins as a foreign antigen to stimulate T cell responses including polyfunctional cytokine-secreting $CD4^+$ and $CD8^+$ T cells. As shown in Fig. 3H, significant infiltration of $CD8^+$ T cells (34.6%) was found inside the serum of SV@**MA**(+L) treated mice, much higher than the control mice treated with PBS (6.75%). In the case of $CD4^+$ T cells, the population of $CD4^+$ T cells in the serum of mice treated with PBS was only 18.6%, while 51.8% $CD4^+$ T cells were observed when the mice were administered with SV@**MA**(+L) (Fig. S18, ESI†). The above results showed that SV@**MA** with light irradiation can break the immunological tolerance against VEGFR2 and activate the $CD4^+$ and $CD8^+$ T cells, which can induce a T cell-mediated autoimmune response against VEGFR2 overexpressed in proliferating endothelial cells. The impact of the activated $CD4^+$ and $CD8^+$ T cells on the suppression of angiogenesis through T cell-mediated killing of endothelial cells was further studied. Immunohistochemical staining with an antibody reactive to CD31 was used to identify the microvessels in 4T1 tumors. The number of microvessels in the SV@**MA** (+L) group was observed to be significantly less than the SV@**MA** (−L) and SV (+L) groups (Fig. 3I and J), indicating the important role of the light-controlled gene release ability in anti-angiogenesis. All the above results showed that SV@**MA** could simultaneously remain and proliferate in the tumor tissue and suppress angiogenesis effectively by a T cell-mediated autoimmune response under light irradiation.

The *in vivo* tumor inhibition effect of SV@**MA** was assessed in a 4T1 tumor-bearing BALB/c mouse model by monitoring the tumor volumes. As expected, SV@**MA**(+L) showed excellent efficiency for tumor inhibition as indicated by the best tumor suppression outcome based on the tumor size (Fig. 4A) from mice on day 22. The tumor growth trends of the SV(−L),

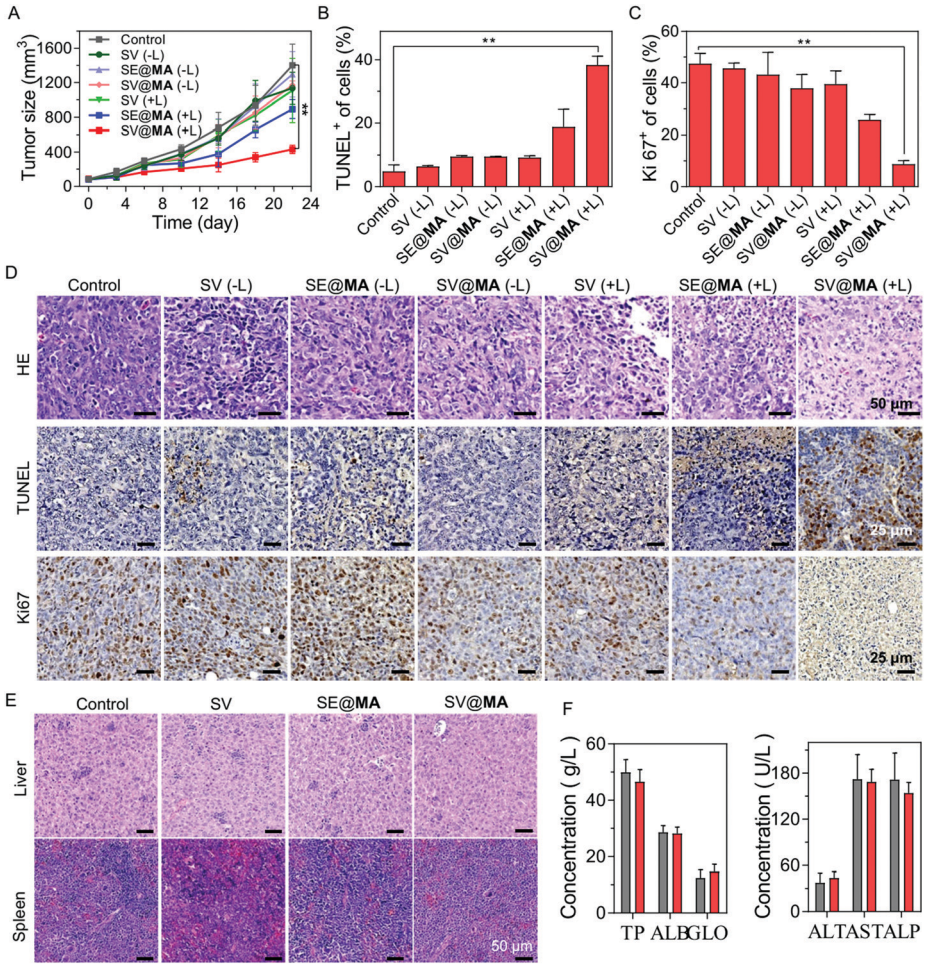

Fig. 4 (A) Tumor growth curve of BALB/c mice with 4T1 xenografts after treatment with different formulations (n = 5). Quantification analyses of (B) TUNEL and (C) Ki-67 of tumor tissues from BALB/c mice after different treatments. (D) HE, TUNEL and Ki-67 analyses of tumor tissues of BALB/c mice bearing 4T1 tumors after different treatments. (E) HE analyses of liver and spleen tissues of BALB/c mice bearing 4T1 tumors after different treatments. (F) Liver and renal function results of mice administered with PBS (gray) or SV@**MA** (red) (n = 3).

SE@**MA**(−L), SV@**MA**(−L) and SV(+L) groups were similar to that of the PBS control, suggesting a poor anti-tumor effect during the treatment. Furthermore, the immumohistochemical staining results, such as terminal deoxynucleotidyl transferase dUTP nick end labeling (TUNEL) (Fig. 4B and D), Ki67 assay staining (Fig. 4C and D) and hematoxylin–eosin (H&E) (Fig. 4D), of tumor tissues from mice after the specified treatment further confirmed the prominent anti-tumor performance of SV@**MA**(+L), in which significant cell apoptosis and proliferation inhibition were found as compared with the other treatment groups.

As a bacteria-based therapeutic system, biosafety-related concerns may be raised due to the administered *Salmonella*. Therefore, a series of biosafety tests were conducted. Fig. S19 (ESI†) shows that *Salmonella* in the blood can be effectively cleared within one week. Meanwhile, at day 1, there were bacteria distributed in the liver and spleen *via* blood circulation, but the bacterial concentrations in the liver and spleen were found to be continuously decreasing until undetectable at day 7, showing good biosafety of such an approach. Notably, no obvious body weight loss was observed in all the treatment groups throughout the observation period (Fig. S20, ESI†), indicating low systemic toxicity of SV@**MA** treatment. This was further confirmed by the negligible toxicity found in H&E staining of major organs (the heart, liver, spleen, lungs, and kidneys) (Fig. 4E and Fig. S21, ESI†) and the negligible changes observed in blood biochemistry analysis including liver functions and renal functions (Fig. 4F and Fig. S22, ESI†) of mice on the 22nd day. All the biosafety results demonstrate that the bacteria-based therapy is well-tolerated by animals with excellent biocompatibility as a living bacteria therapeutic system.

Conclusion

In conclusion, we developed a living therapeutic system based on attenuated *Salmonella via* a metabolic engineering method using an AIE photosensitizer to realize light-controlled gene release for breast cancer therapy. The **MA** labeling method had no inhibitory effects on *Salmonella* reproduction, and thus the administered **MA**-engineered *Salmonella* carrying VEGFR2

plasmids was able to be localized in the tumor tissues and continue to colonize and express exogenous genes. Following the treatment schedule, the constructed plasmids could be released into the cytoplasm of the host cells under light irradiation. The expression of the released plasmid was then demonstrated to be capable of blocking immunological tolerance to VEGFR2 and inducing a T cell-mediated autoimmune antiangiogenic response. Through *in vitro* and *in vivo* experiments, prominent tumor suppression performance was validated with our designed living therapeutic system, which is encouraging for broad therapeutic biomedical research fields, especially for cancer treatment. It's noteworthy that the excitation wavelength of **MA** was in the visible region, which limited its light penetration in *in vivo* applications. Future work will focus on the improvement of the metabolic engineering method using two-photon photosensitizers or NIR photosensitizers to further extend the theranostic applications.

Conflicts of interest

There are no conflicts to declare.

Acknowledgements

We thank Singapore National Research Foundation (R279-000-483-281) and NUS (R279-000-482-133) for financial support. This work was also partially supported by the National Natural Science Foundation of China (grant no. 51873185).

Notes and references

1 D. B. Pedrolli, N. V. Ribeiro, P. N. Squizato, V. N. de Jesus, D. A. Cozetto, R. B. Tuma, A. Gracindo, M. B. Cesar, P. J. Freire and A. F. da Costa, *Trends Biotechnol.*, 2019, **37**, 100–115.
2 A. Maxmen, *Nat. Med.*, 2017, **23**, 5–7.
3 S. Chowdhury, S. Castro, C. Coker, T. E. Hinchliffe, N. Arpaia and T. Danino, *Nat. Med.*, 2019, **25**, 1057–1063.
4 N. Bernardes, R. Seruca, A. M. Chakrabarty and A. M. Fialho, *Bioengineered*, 2010, **1**, 178–190.
5 Q. Hu, M. Wu, C. Fang, C. Cheng, M. Zhao, W. Fang, P. K. Chu, Y. Ping and G. Tang, *Nano Lett.*, 2015, **15**, 2732–2739.
6 W. Chen, Z. Guo, Y. Zhu, N. Qiao, Z. Zhang and X. Sun, *Adv. Funct. Mater.*, 2020, **30**, 1906623.
7 V. Singh, P. Schwerk and K. Tedin, *Gut Pathog.*, 2018, **10**, 33.
8 S. Castanheira and F. García-del Portillo, *Front. Cell. Infect. Microbiol.*, 2017, **7**, 432.
9 E. M. Camacho, B. Mesa-Pereira, C. Medina, A. Flores and E. Santero, *Sci. Rep.*, 2016, **6**, 30591.
10 R. Palffy, R. Gardlik, J. Hodosy, M. Behuliak, P. Reško, J. Radvánský and P. Celec, *Gene Ther.*, 2006, **13**, 101–105.
11 S. Pilgrim, J. Stritzker, C. Schoen, A. Kolb-Mäurer, G. Geginat, M. J. Loessner, I. Gentschev and W. Goebel, *Gene Ther.*, 2003, **10**, 2036–2045.
12 N. Souders, T. Verch and Y. Paterson, *DNA Cell Biol.*, 2006, **25**, 142–151.
13 N. Bernardes, A. M. Chakrabarty and A. M. Fialho, *Appl. Microbiol. Biotechnol.*, 2013, **97**, 5189–5199.
14 S. Zhou, C. Gravekamp, D. Bermudes and K. Liu, *Nat. Rev. Cancer*, 2018, **18**, 727–743.
15 B. Kim, S. Suvas, P. P. Sarangi, S. Lee, R. A. Reisfeld and B. T. Rouse, *J. Immunol.*, 2006, **177**, 4122–4131.
16 W. Song, Q. Sun, Z. Dong, D. Spencer, G. Nunez and J. Nör, *Gene Ther.*, 2005, **12**, 320–329.
17 Y. Li, M. Wang, H. Li, K. D. King, R. Bassi, H. Sun, A. Santiago, A. T. Hooper, P. Bohlen and D. J. Hicklin, *J. Exp. Med.*, 2002, **195**, 1575–1584.
18 J. Liu, Y. Wei, L. Yang, X. Zhao, L. Tian, J. Hou, T. Niu, F. Liu, Y. Jiang and B. Hu, *Blood*, 2003, **102**, 1815–1823.
19 Y. Wei, Q. Wang, X. Zhao, L. Yang, L. Tian, Y. Lu, B. Kang, C. Lu, M. Huang and Y. Lou, *Nat. Med.*, 2000, **6**, 1160–1166.
20 F. Hu, G. Qi, D. Mao, S. Zhou, M. Wu, W. Wu and B. Liu, *Angew. Chem.*, 2020, **59**, 9288–9292.
21 D. Wang, M. M. Lee, G. Shan, R. T. Kwok, J. W. Lam, H. Su, Y. Cai and B. Z. Tang, *Adv. Mater.*, 2018, **30**, 1802105.
22 J. H. Zheng and J.-J. Min, *Chonnam Med. J.*, 2016, **52**, 173–184.
23 S. Rius-Rocabert, F. Llinares Pinel, M. J. Pozuelo, A. García and E. Nistal-Villan, *FEMS Microbiol. Lett.*, 2019, **366**, fnz136.
24 A. G. Niethammer, R. Xiang, J. C. Becker, H. Wodrich, U. Pertl, G. Karsten, B. P. Eliceiri and R. A. Reisfeld, *Nat. Med.*, 2002, **8**, 1369–1375.
25 H. Zhou, Y. Luo, M. Mizutani, N. Mizutani, R. A. Reisfeld and R. Xiang, *Blood*, 2005, **106**, 2026–2032.
26 J. Lyons, B. Sheahan, S. Galbraith, R. Mehra, G. Atkins and M. Fleeton, *Gene Ther.*, 2007, **14**, 503–513.
27 S. Xu, Y. Duan and B. Liu, *Adv. Mater.*, 2020, **32**, 1903530.
28 H. Su, C. Chou, D. Hung, S. Lin, I. Pao, J. Lin, F. Huang, R. Dong and J. Lin, *Biomaterials*, 2009, **30**, 5979–5987.
29 H. Jia, Y. Zhu, Z. Chen and F. Wu, *ACS Appl. Mater. Interfaces*, 2017, **9**, 15943–15951.
30 M. Wu, W. Wu, Y. Duan, X. Li, G. Qi and B. Liu, *Chem. Mater.*, 2019, **31**, 7212–7220.
31 C. H. Jones, S. Rane, E. Patt, A. Ravikrishnan, C. Chen, C. Cheng and B. A. Pfeifer, *Mol. Pharmaceutics*, 2013, **10**, 4301–4308.
32 S. Xie, L. Zhao, X. Song, M. Tang, C. Mo and X. Li, *J. Controlled Release*, 2017, **268**, 390–399.
33 C. Clairmont, K. Lee, J. Pike, M. Ittensohn, K. Low, J. Pawelek, D. Bermudes, S. Brecher, D. Margitich and J. Turnier, *J. Infect. Dis.*, 2000, **181**, 1996–2002.
34 M. Wu, X. Liu, H. Bai, L. Lai, Q. Chen, G. Huang, B. Liu and G. Tang, *ACS Appl. Mater. Interfaces*, 2019, **11**, 9850–9859.
35 R. Heidenreich, A. Kappel and G. Breier, *Cancer Res.*, 2000, **60**, 6142–6147.
36 D. J. Hicklin, F. M. Marincola and S. Ferrone, *Mol. Med. Today*, 1999, **5**, 178–186.
37 X. Lu, X. Jiang, R. Liu and S. Zhang, *Vaccine*, 2008, **26**, 5352–5357.

